doi:10.1016/j.jmb.2006.06.054 J. Mol. Biol. (2006) 361, 888–897

JMB

Available online at www.sciencedirect.com

ScienceDirect

ELSEVIER

Crystal Structure of a Non-discriminating Glutamyl-tRNA Synthetase

Jörg O. Schulze[1], Ava Masoumi[2], Daniel Nickel[1], Martina Jahn[2] Dieter Jahn[2], Wolf-Dieter Schubert[1] and Dirk W. Heinz[1]*

[1]*Division of Structural Biology German Research Centre for Biotechnology (GBF) Mascheroder Weg 1 D-38124 Braunschweig Germany*

[2]*Institute of Microbiology Technical University Braunschweig, Spielmannstr. 7 D-38106 Braunschweig Germany*

**Corresponding author*

Error-free protein biosynthesis is dependent on the reliable charging of each tRNA with its cognate amino acid. Many bacteria, however, lack a glutaminyl-tRNA synthetase. In these organisms, $tRNA^{Gln}$ is initially mischarged with glutamate by a non-discriminating glutamyl-tRNA synthetase (ND-GluRS). This enzyme thus charges both $tRNA^{Glu}$ and $tRNA^{Gln}$ with glutamate. Discriminating GluRS (D-GluRS), found in some bacteria and all eukaryotes, exclusively generates Glu-$tRNA^{Glu}$. Here we present the first crystal structure of a non-discriminating GluRS from *Thermosynechococcus elongatus* (ND-$GluRS_{Tel}$) in complex with glutamate at a resolution of 2.45 Å. Structurally, the enzyme shares the overall architecture of the discriminating GluRS from *Thermus thermophilus* (D-$GluRS_{Tth}$). We confirm experimentally that $GluRS_{Tel}$ is non-discriminating and present kinetic parameters for synthesis of Glu-$tRNA^{Glu}$ and of Glu-$tRNA^{Gln}$. Anticodons of $tRNA^{Glu}$ ($^{34}C/UUC^{36}$) and $tRNA^{Gln}$ ($^{34}C/UUG^{36}$) differ only in base 36. The pyrimidine base of C36 is specifically recognized in D-$GluRS_{Tth}$ by the residue Arg358. In ND-$GluRS_{Tel}$ this arginine residue is replaced by glycine (Gly366) presumably allowing both cytosine and the bulkier purine base G36 of $tRNA^{Gln}$ to be tolerated. Most other ND-GluRS share this structural feature, leading to relaxed substrate specificity.

Keywords: aminoacylation; mischarging; misacylation; anticodon recognition; glutaminyl-tRNA synthetase

Introduction

The faithful translation of genetic information requires that transfer RNA (tRNA) is reliably loaded with its cognate amino acid before reaching the ribosome during protein biosynthesis. This is ensured by a set of aminoacyl-tRNA synthetases (AARS) each of which catalyzes the aminoacylation of a specific tRNA. Based on their distinct ATP-binding cores, AARS fall into two classes of ten enzymes each.[1] Active sites of class I enzymes (including GluRS and GlnRS) involve a parallel β-sheet Rossmann fold with two conserved amino acid motifs for ATP binding. Class II enzymes (AspRS, AsnRS and others) exhibit a central seven-stranded, antiparallel β-sheet with three conserved motifs.[1]

tRNA aminoacylation is a two-step event. First, the AARS activates the amino acid using ATP and Mg^{2+} to yield an enzyme-bound, high-energy aminoacyl adenylate intermediate. Then, in a second step, the aminoacyl moiety is transferred to the 3′-terminal adenosine of the cognate tRNA. In GluRS, GlnRS and ArgRS, the first step occurs only in the presence of the tRNA.[2]

AARS reliably discriminate between different tRNAs, such that the 20 proteinogenic amino acid residues generally require a corresponding number of tRNAs and AARS.[3] Numerous organisms, however, possess fewer than these 20 AARS.[4] In particular, glutaminyl-tRNA, asparaginyl-tRNA[5] and cysteinyl-tRNA[6] synthetases may be affected. Thus, all archaea,[7] most bacteria, as well as mitochondria and chloroplasts[8] lack glutaminyl-tRNA synthetase (GlnRS). In exchange, a non-discriminating glutamyl-tRNA synthetase (ND-GluRS) charges both $tRNA^{Glu}$ and $tRNA^{Gln}$ with glutamate (Scheme 1).[9] The resulting misacylated

Abbreviations used: AARS, aminoacyl-tRNA synthetase; D, discriminating; ND, non-discriminating; AdT, amidotransferase; *Tel*, *Thermosynechococcus elongatus*; *Tth*, *Thermus thermophilus*; *Eco*, *Escherichia coli*; CP, connective polypeptide; SC, stem contact.

E-mail address of the corresponding author: Dirk.Heinz@gbf.de

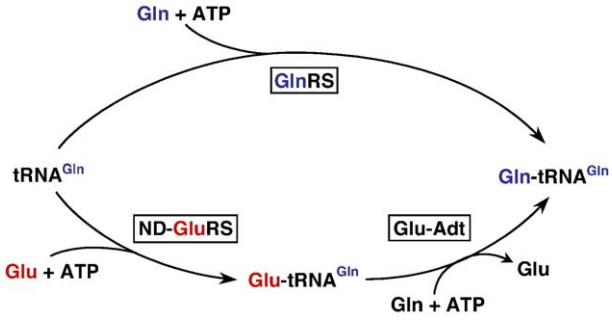

Scheme 1. Production of Gln-tRNA^{Gln} *in vivo*. Eukaryotes and some bacteria produce Gln-tRNA^{Gln} directly using a dedicated GlnRS (top). Most bacteria, however, lack GlnRS. Instead they possess a non-discriminating GluRS (ND-GluRS) that charges both tRNA^{Glu} and tRNA^{Gln} with glutamate (bottom). Misacylated Glu-tRNA^{Gln} is subsequently amidated to Gln-tRNA^{Gln} by a tRNA-dependent amidotransferase (Glu-AdT or GatCAB) that utilizes free glutamine hydrolyzing it to glutamate.

Glu-tRNA^{Gln} is then converted to Gln-tRNA^{Gln} by a tRNA-dependent amidotransferase (AdT) through the addition of amide to the glutamate. The indirect synthesis known as the transamidation pathway is the more ancient way of producing Gln-tRNA^{Gln}.[10]

The anticodon-binding domains of bacterial and archaeal/eukaryotic GluRS differ structurally. While the former has an all α-helical topology, the secondary structure of the latter exclusively involves β-strands.[11] Sequence comparisons and the all-β anticodon-binding domain indicate that GlnRS evolved from GluRS in eukaryotes shortly after the archaea/eukarya divide.[12] Some bacterial species such as *Thermus*, *Deinococcus* and proteobacteria of the β and γ-families then presumably acquired GlnRS by horizontal gene transfer.[13]

Here we present the first crystal structure of a non-discriminating GluRS from the thermophilic cyanobacterium *Thermosynechococcus elongatus* (ND-GluRS$_{Tel}$) at 2.45 Å resolution. The principal structural feature distinguishing ND-GluRS$_{Tel}$ from discriminating GluRS from *Thermus thermophilus* (D-GluRS$_{Tth}$)[11] is the substitution of an arginine residue by glycine in the anticodon-binding domains, presumably to allow the bulky base G36 of the tRNA^{Gln} anticodon to be accommodated. Moreover, we present catalytic constants for charging Glu-tRNA^{Glu} and Glu-tRNA^{Gln} confirming GluRS$_{Tel}$ to be non-discriminating.

Results

GluRS from *T. elongatus* is non-discriminating

The genome[14] of the thermophilic cyanobacterium *T. elongatus* does not include a gene encoding a glutaminyl-tRNA synthetase (GlnRS).[15] Instead, the genes *gatC*, *gatA* and *gatB* for the heterotrimeric amidotransferase Glu-AdT (or GatCAB)[16] are present.[15] Glutamyl-tRNA synthetase of *T. elongatus* (GluRS$_{Tel}$) is thus presumably non-discriminating, acylating both tRNA^{Glu} and tRNA^{Gln} followed by the conversion of misacylated Glu-tRNA^{Gln} to Gln-tRNA^{Gln} by GatCAB.

To unambiguously demonstrate the non-discriminating character of GluRS$_{Tel}$, recombinant purified enzyme and mature tRNA^{Glu} and tRNA^{Gln} purified from *T. elongatus* extracts[17] were used in aminoacylation assays. Northern dot-blot analyses confirm the complete separation of the extract-derived tRNAs (data not shown). Glutamylation of tRNA^{Glu} and tRNA^{Gln} were quantified by iterative Lineweaver–Burk analysis over a substrate range from 0.2 μM to 7 μM (Table 1). The kinetic data for misacylation of tRNA^{Gln} by GluRS$_{Tel}$ were found to be $K_m = 3.7(\pm 0.4)$ μM and $k_{cat} = 0.036\ (\pm 0.003)\ s^{-1}$ yielding a $k_{cat}/K_m = 9.7(\pm 0.7)\ s^{-1}mM^{-1}$. Corresponding values for tRNA^{Glu} are $K_m = 0.79(\pm 0.07)$ μM, $k_{cat} = 0.1\ (\pm 0.03)\ s^{-1}$ and $k_{cat}/K_m = 126(\pm 0.5)\ s^{-1}mM^{-1}$. Glutamylation of tRNA^{Glu} is thus 13-fold more efficient (k_{cat}/K_m) than that of tRNA^{Gln}.

By comparison, discriminating GluRS from *Escherichia coli* (D-GluRS$_{Eco}$) is unable to misacylate the non-cognate tRNA^{Gln}. A K_m of 190 μM and a k_{cat} of $7 \times 10^{-5}\ s^{-1}$ yield a k_{cat}/K_m value of $10^{-8}\ s^{-1}mM^{-1}$, indicating that tRNA^{Gln} does not serve as a natural substrate for D-GluRS$_{Eco}$.[18] The corresponding situation for aspartyl-tRNA synthetase (AspRS) has been analyzed for the enzymes of *Thermus thermophilus*,[19] which express both a non-discriminating AspRS (ND-AspRS2), as well as a discriminating AspRS (D-AspRS1) and a dedicated AsnRS. While the efficiency (k_{cat}/K_m) for aminoacylation of tRNA^{Asn} and tRNA^{Asp} by D-AspRS1 differs 2250-fold, the difference for ND-AspRS2 only amounts to a factor of 2.[19]

Structure of ND-GluRS$_{Tel}$

The crystal structure of ND-GluRS$_{Tel}$ (54.4 kDa) was solved by molecular replacement using discriminating GluRS from *T. thermophilus* (D-GluRS$_{Tth}$; PDB-code 1GLN), which shares a sequence identity of 37% to GluRS$_{Tel}$ as search model, and refined to a resolution of 2.45 Å. The asymmetric unit contains two molecules. All 485 amino acid residues of monomer A are well resolved, while a further four residues of the C-terminal His$_6$-tag are visible in the electron density of monomer B. Data collection and refinement statistics are summarized in Table 2.

ND-GluRS$_{Tel}$ is an elongated, slightly curved molecule, 110 Å in length and 35–40 Å in width. The modular protein consists of five domains (Figures 1 and 2(a)). The N-terminal, catalytic domain (green in Figure 1) has a dinucleotide

Table 1. Catalytic constants for Glu-tRNA^{Glu} and Glu-tRNA^{Gln} formation by non-discriminating GluRS$_{Tel}$

tRNA	K_m (μM)	k_{cat} (s^{-1})	k_{cat}/K_m ($s^{-1}\ mM^{-1}$)
Glu-tRNA^{Glu}	0.79±0.07	0.1±0.03	126±0.5
Glu-tRNA^{Gln}	3.7±0.4	0.036±0.003	9.7±0.7

Table 2. Data collection and structure refinement

A. *Data collection*	
Unit cell dimensions, *a*, *b*, *c* (Å)	36.2, 99.6, 182.4
Space group	$P2_1$
Wavelength (Å)	0.90
Number of unique reflections	51,842
Resolution range (Å)	50-2.45 (2.55-2.45)
Completeness of data (%)	96.9 (91.2)
Redundancy	2.8 (2.4)
R_{merge} (%)	11.2 (42.4)
I/σ	11.2 (3.2)
B. *Refinement statistics*	
Maximum resolution (Å)	2.45 (2.51-2.45)
No. of atoms: protein, water	7743, 321
Monomers per asymmetric unit	2
R-factor (%)	18.1 (26.4)
R_{free} (%)	24.8 (32.2)
Average *B*-factor (Å^2)	17.7
r.m.s.d. bond length (Å)	0.02
r.m.s.d. bond angles (°)	1.50
Ramachandran plot[a]	95.5/4.5/0/0

Values in parentheses refer to the shell of highest resolution.
[a] PROCHECK[42]: most favored/additionally allowed/generously allowed/disallowed regions.

binding or Rossmann fold characterized by a central five-stranded, parallel β-sheet, flanked by α-helices. A deep pocket accommodates the active site, including binding sites for glutamate and the acceptor end of tRNA. The conserved ATP-binding motifs, HIGT and KLSKR, respectively, located at the N-terminal end of α-helix αA and in a loop between β-strand β11 and helix αI, form part of the active site pocket. The acceptor binding or connective polypeptide (CP) domain is sequentially inserted into the catalytic domain, dividing the latter into two subdomains. The acceptor binding domain, comprising three α-helices and two antiparallel β-sheets of four and two strands, respectively, causes the helical tRNA acceptor end to change its conformation during binding to allow the 3′ end to fit into the active site.[20] The two N-terminal domains are followed by three α-helical domains: The stem contact (SC) domain (four α-helices) and two anticodon-binding domains, a three-helix bundle and a six-helix cage, respectively. The crystallographically independent monomers A and B are structurally largely identical. Their modular architecture, however, allows monomer A to bend slightly more than monomer B. The difference leads to a root-mean-square deviation (r.m.s.d.) of 0.9 Å for the Cα atoms of both molecules.

A Zn^{2+} binding site involving the so-called SWIM motif Cys-x-Cys-x_{24}-Cys-x-His has been identified in D-GluRS$_{Eco}$ by extended X-ray absorption fine structure (EXAFS) analysis and site-directed mutagenesis studies.[21,22] It serves to stabilize a subdomain of the CP domain required to correctly position the tRNA acceptor end in the active site. Though ND-GluRS$_{Tel}$ bears a similar motif (Cys98-x-Cys100-x_{24}-His125-x-His127) and 250 μM zinc acetate was added to the crystallization drops, Zn^{2+} was not observed to bind. Instead the side-chains of Cys98, Cys100 and His125 are in mutual van-der-Waals contact while His127 is structurally removed and points away from the other potential ligands. Aminoacylation assays indicate that ND-GluRS$_{Tel}$ does not require Zn^{2+}, in contrast to D-GluRS$_{Eco}$.[21] Phylogenetic studies correspondingly reveal frequent differences in the proposed Zn^{2+} binding site of closely related species indicating a possible rapid evolution of this regulatory element.[22]

Glutamate recognition

In ND-GluRS$_{Tel}$ monomer A, a glutamate substrate molecule is bound within a positively charged pocket of the active site (Figure 3(a)). Its γ-carboxyl group forms two salt bridges to the guanidinium groups of Arg6 and Arg210 and a hydrogen bond to the Tyr192 hydroxyl group. The α-carboxyl group is involved in a hydrogen bond or salt bridge to atom His214-N$^{\delta 1}$. The amino acid specificity of GluRS is thus ensured by the glutamate binding site recognizing substrates of suitable size and charge distribution.

Discussion

Structural differences between ND-GluRS$_{Tel}$ and D-GluRS$_{Tth}$

As indicated by the sequence identity of 37%, ND-GluRS$_{Tel}$ is structurally similar to D-GluRS$_{Tth}$ (Figure 2). The three N-terminal domains show a particularly high degree of conservation (sequence identity of 44%) with extended stretches of conserved residues being especially apparent in the catalytic domain. Correspondingly, these domains of ND-GluRS$_{Tel}$ and D-GluRS$_{Tth}$ align particularly well. A sequence identity of only 25% in the anticodon-binding domains results in distinct differences reflecting their structural rather than functional role.[23] Thus, only individual residues of the hydrophobic core and the C terminus of αS are conserved. Many α-helices are displaced while some loops adopt distinctly diverging conformations. The superposition of ND-GluRS$_{Tel}$ monomer A on apo (PDB code 1GLN)[11] and on tRNA-bound D-GluRS$_{Tth}$ (PDB code 1N77)[2] yield r.m.s.d. values of 3.3 (2.9 for monomer B) and 3.0 (2.9) Å for 459 common Cα atoms. These deviations primarily result from subtle domain reorientations in different GluRS molecules.

Insertions/deletions in primary structure give rise to the most prominent structural differences between ND-GluRS$_{Tel}$ and D-GluRS$_{Tth}$. The first, by sequence (Δ1 in Figure 2(a)), involves eight residues inserted between β3 and αC of the catalytic domain, and mainly occurs in GluRS of γ-proteobacteria and spirochaetes. Δ1 creates a bulge in D-GluRS$_{Tth}$ not involved in tRNA binding or catalysis and its absence in ND-GluRS$_{Tel}$ presumably has no functional implications. The second insertion, Δ2, involves six amino acid residues in the acceptor-

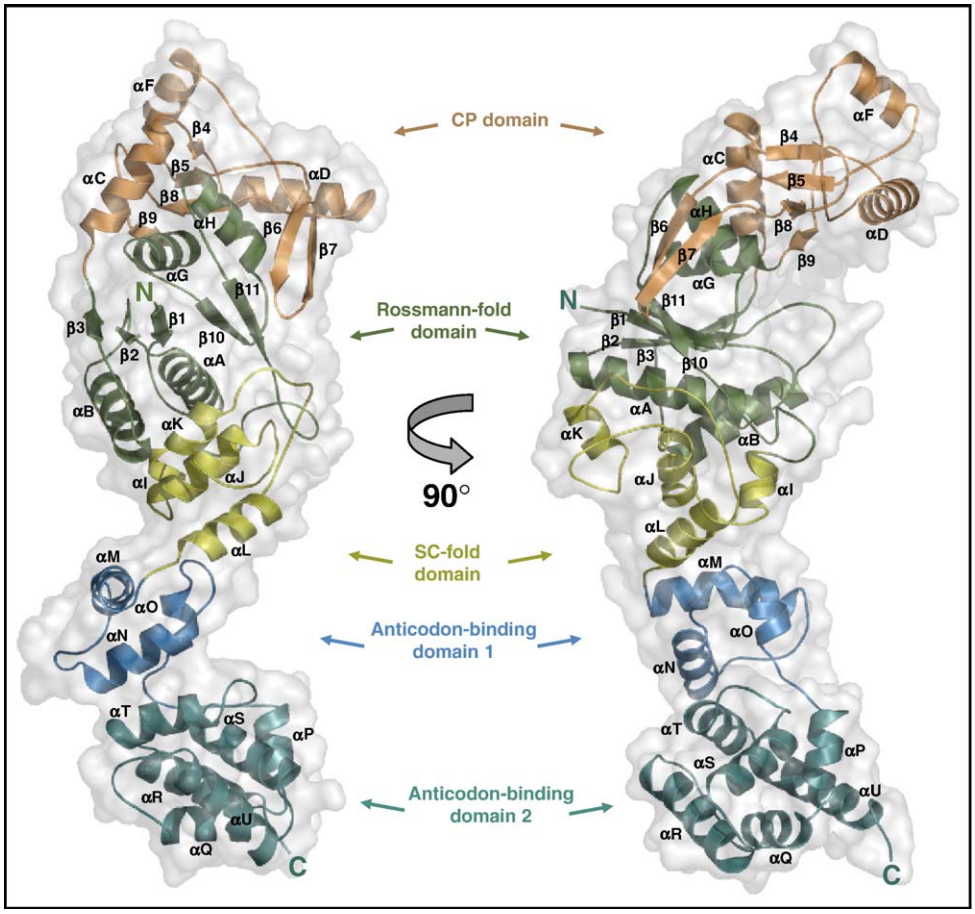

Figure 1. Cartoon representation of non-discriminating GluRS from *T. elongatus* (ND-GluRS$_{Tel}$) with transparent surface. The right view is rotated by 90° relative to the left view. The catalytic domain is depicted in green, the connective peptide (CP) domain in orange, the stem contact (SC)-fold domain in yellow, and anticodon-binding domains 1 and 2 in light blue and cyan, respectively. All molecular depictions were produced using PyMOL [http://www.pymol.sourceforge.net].

binding domain. It is present in all bacterial GluRS enzymes (including ND-GluRS$_{Tel}$) except those of *Deinococcus/Thermus* species, which are discriminating (D-GluRS$_{Tth}$). Δ2 elongates α-helix αD C-terminally by one turn and lengthens the adjoining loop. Δ3, an insertion of five residues exclusively observed in cyanobacterial GluRS, serves to lengthen the loop between β8 (CP domain) and αG (catalytic domain) in ND-GluRS$_{Tel}$ forcing αF to shift by ~7 Å compared to D-GluRS$_{Tth}$. Neither Δ3 nor αF participate in tRNA binding or catalysis. Two minor insertions (Δ4 and Δ5) located in the anticodon-binding domains again extend two loops on the side of the enzyme not involved in tRNA-binding, while Δ6 elongates the C terminus of ND-GluRS$_{Tel}$ by six amino acid residues.

Substrate recognition in the active site

A model of tRNA^{Glu}-bound ND-GluRS$_{Tel}$ was obtained by superimposing tRNA^{Glu}-bound D-GluRS$_{Tth}$[2] on ND-GluRS$_{Tel}$. In this model, the elongated protein forms a continuous interaction interface with one side of the L-shaped tRNA extending from the anticodon loop to the acceptor end.

The acceptor-end of tRNA^{Glu} structurally matches its binding site created by the catalytic and acceptor-binding domains (Figure 3(b)). In direct analogy to D-GluRS$_{Tth}$,[2] a protrusion of the CP domain presumably unwinds the helical acceptor-end of the unbound tRNA inducing the 3′ end to adopt a hairpin conformation required to fill the active site. Base C74 would then be accommodated within a pocket in the CP domain, while A73, C75 and A76 will stack upon His214 and Tyr192.

Insertion Δ2 (see above) increases the size of the protrusion separating the tRNA 5′ and 3′ ends in ND-GluRS$_{Tel}$ compared to D-GluRS$_{Tth}$. This extension is common to all non-discriminating, bacterial GluRS, but not the discriminating *Deinococcus/Thermus* enzymes. The insertion would thus appear to be required for tRNA^{Gln} but not tRNA^{Glu} binding.

In D-GluRS$_{Tth}$ ATP initially binds to a "non-productive" sub-site spatially removed from the second substrate glutamate.[2] Upon tRNA-binding, ATP moves to the "productive" sub-site reacting with glutamate to yield the intermediate glutamyl-AMP, which aminoacylates the tRNA. Most active-site residues are conserved in ND-GluRS$_{Tel}$,

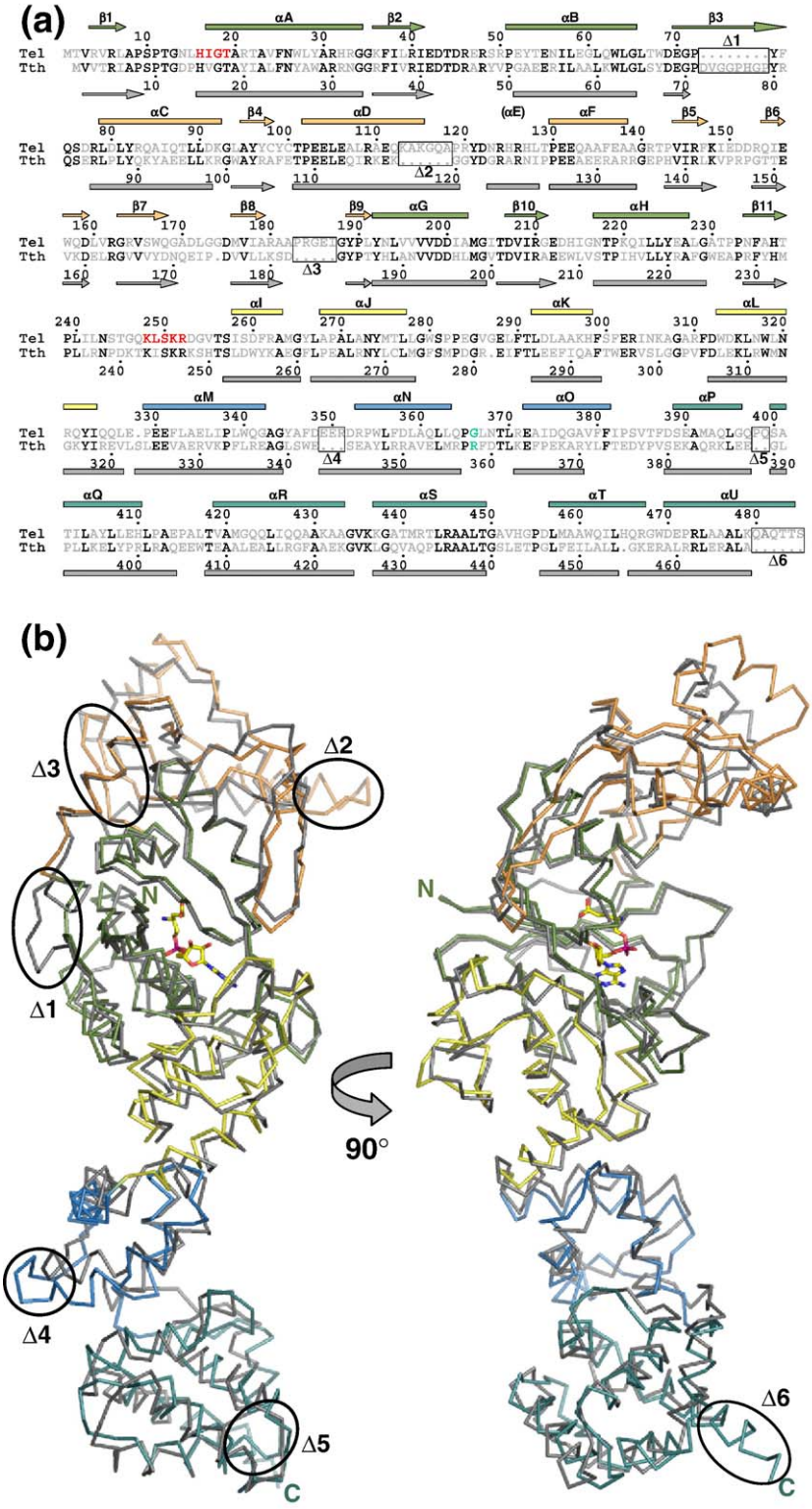

Figure 2. Comparison of ND-GluRS$_{Tel}$ and discriminating GluRS from *T. thermophilus* (D-GluRS$_{Tth}$). (a) Sequence alignment with conserved residues shown in black, all others in gray. Rectangles and arrows (colors as in Figure 1) above the alignment indicate α-helices and β-strands, respectively. Red letters highlight the ATP-binding motifs and cyan letters the residues mainly responsible for (non-)discrimination. Insertions/deletions are boxed and marked by a sequentially numbered Δ. (b) Structural comparison as a Cα trace representation. ND-GluRS$_{Tel}$ is colored as in Figure 1, while D-GluRS$_{Tth}$ is depicted in gray. The two views are rotated by 90°. Insertions and deletions are highlighted by black ellipses.

indicating that the described mechanism is similarly conserved.

Recognition of tRNA^{Glu} and tRNA^{Gln}

In the complex of tRNA^{Glu}/D-GluRS$_{Tth}$, the anticodon loop of tRNA^{Glu} adopts a U-turn structure while its minor groove interacts with the two anticodon-binding domains.[24] Our model indicates that this occurs in ND-GluRS$_{Tel}$ as well. The anticodon-binding domain of ND-GluRS$_{Tel}$ forms a cavity similar to the one accommodating the stacked anticodon nucleotides C34 and U35 in D-GluRS$_{Tth}$ (Figure 4). These bases are thus recognized by the helix-loop-helix structure of αM, αM-αN and αN (residues 437–458 in ND-GluRS$_{Tel}$). C34 would laterally interact with the hydrophobic side chains of Met441, Leu457 and Met458 while atoms O2 and

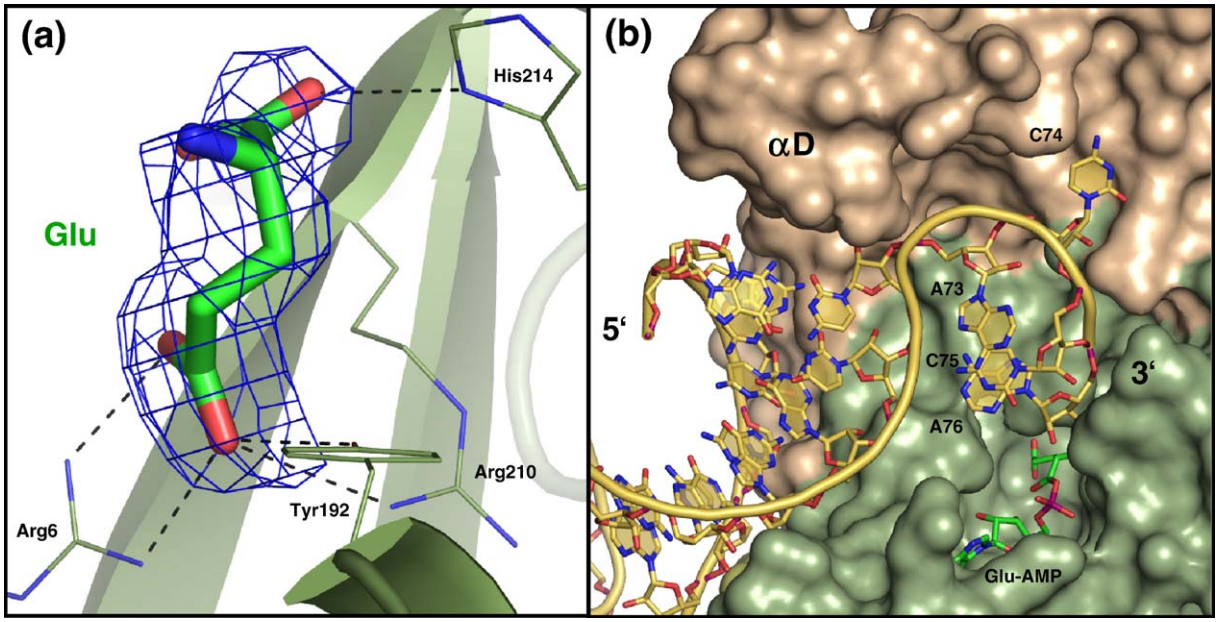

Figure 3. Substrate recognition in the active site of ND-GluRS$_{Tel}$. (a) Electron density of the substrate glutamate ($|2F_O-F_C|$ map contoured at 1σ). Residues involved in binding are shown as sticks. (b) Model of the acceptor end of tRNA^{Glu} of *T. thermophilus* and the reaction intermediate glutamyl-AMP in the active site of ND-GluRS$_{Tel}$. The enzyme is shown in surface representation with the catalytic domain in green and the connective peptide (CP) domain in light brown. tRNA^{Glu} and glutamyl-AMP are depicted in stick representation with carbon atoms in bronze and green, respectively. Oxygen atoms are rendered in red, nitrogen atoms in blue, and phosphorus in purple.

N3 form hydrogen bonds to the side-chain guanidinium group of Arg445 and the main-chain amide group of Leu447, respectively. In *E. coli*, a modified uridine at position 34 (5-methylaminomethyl-2-thiouridine, mnm^{5}s^{2}U) is a major identity element for tRNA^{Glu} recognition by GluRS.[25] Though the modification of this base in tRNA^{Glu} from *T. elongatus* has not been analyzed, a modified mnm^{5}s^{2}U34 could feasibly be accommodated allowing for a hydrogen bond between the 2-thiocarbonyl moiety and Arg445, while the 5-methylaminomethyl group facing away from the protein would not incur any steric clashes. Our model indicates that U35 would be recognized through hydrogen bonds U35-O2—Gly454-O, U35-N3—Gly454-N, and U35-O2—Val452-O.

The anticodons of tRNA^{Glu} (^{34}C/UUC^{36}) and tRNA^{Gln} (^{34}C/UUG^{36}) differ only with respect to base 36. Discrimination and non-discrimination in GluRS must, therefore, be linked to differences in recognition of this nucleotide. In D-GluRS$_{Tth}$,[19] the guanidinium side-chain Arg358 of the first anticodon-binding domain specifically recognizes the pyrimidine base C36 through hydrogen bonds to O2 and N3 (Figure 4(d)). This arginine residue is replaced by glycine (G366) in ND-GluRS$_{Tel}$, abrogating recognition of C36 of tRNA^{Glu} and creating a cavity that allows the larger purine base G36 of tRNA^{Gln} to be easily accommodated. While binding of tRNA^{Gln} to GlnRS requires a rearrangement of the three anticodon bases allowing each to bind to a separate binding pocket,[26] the binding to ND-GluRS$_{Tel}$, by contrast, assumes the anticodon bases of tRNA^{Gln} to stack as documented for tRNA^{Glu}. Since this is presumably the structure of tRNA^{Gln} in solution, a rearrangement of nucleotides would not be required during binding.

Discrimination versus non-discrimination by GluRS

Evolutionarily, non-discrimination of tRNA^{Glu} and tRNA^{Gln} by GluRS is more ancient, while discrimination appears first to have occurred in eukaryotes following the divergence of GlnRS from non-discriminating GluRS.[13] The transfer of GlnRS to individual bacteria allowed the GluRS to become discriminating by additionally distinguishing anticodon base 36 through an additional binding site in the first anticodon-binding domain. Non-discrimination by GluRS thus represents the standard situation, while discrimination required a dedicated fine-tuning of the enzyme to ensure that the previously acceptable G34 of tRNA^{Gln} is reliably rejected.

Sequence alignments of non-discriminating GluRS indicate that Gly366 of ND-GluRS$_{Tel}$ is conserved in *Caulobacter crescentus*, *Fusobacterium nucleatum* and GluRS1 of *Thermoanaerobacter tengcongensis* (incorrectly annotated as GluRS2 in UniProt), but replaced by serine in cyanobacterial GluRS or by glutamine/glutamate in firmicutes (e.g. *Bacillus*, *Lactobacillus* or *Mycoplasma*) GluRS. The fact that a glycine or glutamine residue in this position is not sufficient to allow discrimination is illustrated by the loss of discrimination in the mutant R358Q of D-GluRS$_{Tth}$.[24]

Interestingly, an arginine residue is observed at the position corresponding to Gly366 of ND-

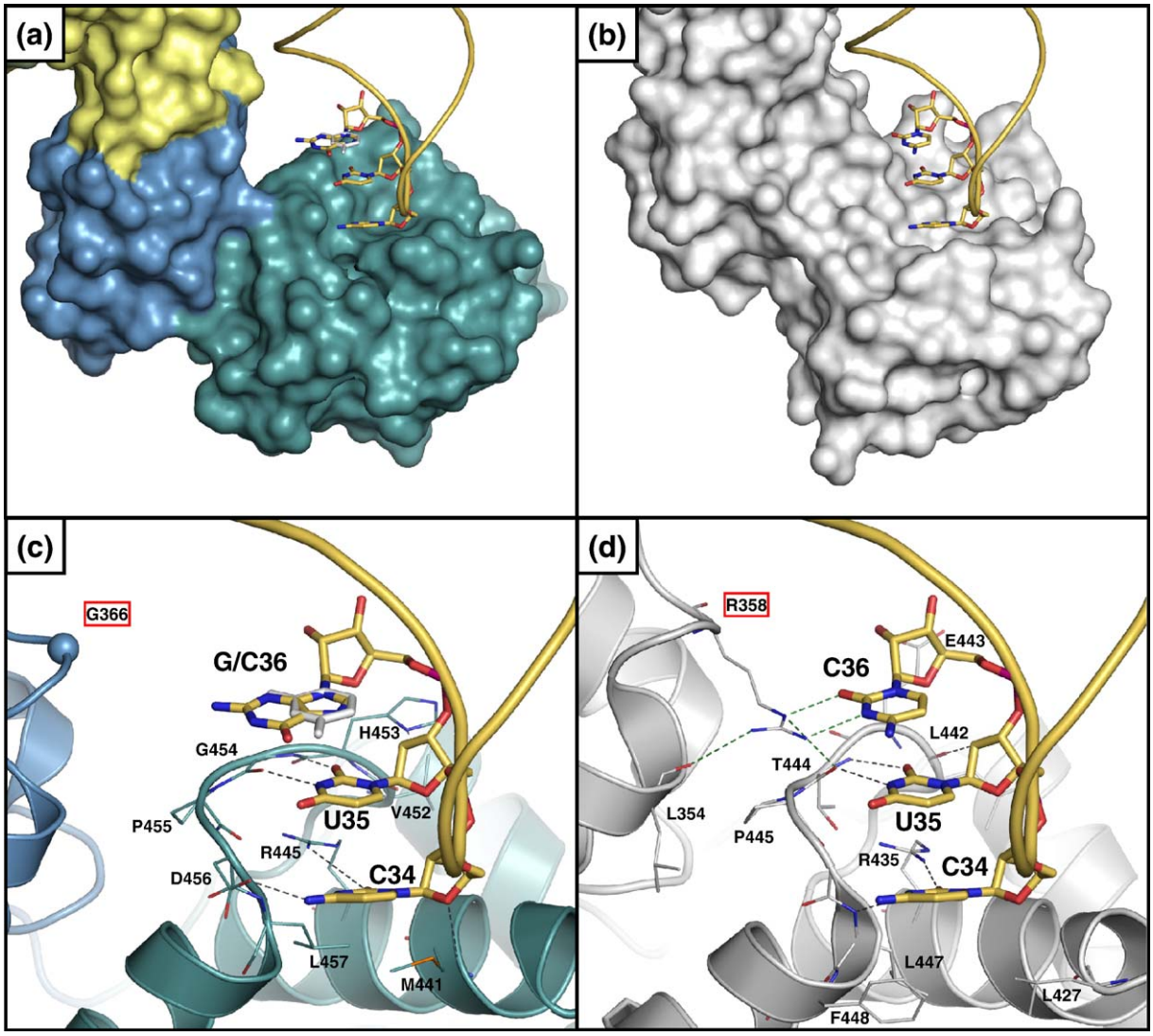

Figure 4. Structural comparison of the anticodon-binding domains of ND-GluRS$_{Tel}$ ((a) and (c)) and D-GluRS$_{Tth}$ ((b) and (d)). ND-GluRS$_{Tel}$ is colored as described for Figure 1, D-GluRS$_{Tth}$ in gray. The tRNA backbone and the three anticodon nucleotides are depicted in bronze. (a) Surface representation of ND-GluRS$_{Tel}$ with modeled tRNA$^{Glu/Gln}$ and (b) D-GluRS$_{Tth}$ with tRNA^{Glu} (PDB code 1N77).[2] (c) Cartoon representation of the anticodon recognition sites of ND-GluRS$_{Tel}$ and (d) D-GluRS$_{Tth}$. For clarity only residues in contact with the anticodon nucleotides are shown (thin sticks).

GluRS$_{Tel}$ (or Arg358 of D-GluRS$_{Tth}$) in actinobacteria, spirchaetes and chlamydiae. However, these species lack a gene for GlnRS but do carry *gatCAB*,[15] implying their GluRS to be non-discriminating. An arginine at this position in itself therefore does not suffice to ensure discrimination. In tRNA-free D-GluRS$_{Tth}$ Arg358 is stabilized by a salt bridge to Glu443. Upon tRNA binding, this interaction is disrupted. Glu443 interacts with the tRNA backbone while Arg358 forms a stacking interaction with Pro357 and a hydrogen bond to Leu354-O. The intricate stabilization of arginine in D-GluRS$_{Tth}$ indicates this to be crucial to discrimination. This inference is supported by the fact that non-discriminating GluRS with an arginine in position 366 (D-GluRS$_{Tel}$) never possess a glutamate at position 443.

Yet another variation is observed in some proteobacteria such as *Helicobacter*, *Rickettsia* or *Bartonella*. These species express both a non-discriminating GluRS1 and a discriminating GluRS2.[15] In all corresponding GluRS2, an arginine residue is observed at the critical discrimination position. GluRS1 all feature an asparagine or glutamate at this position.

Comparison with non-discriminating aspartyl-tRNA synthetase

The anticodons of tRNA^{Asp} (^{34}GUC^{36}) and tRNA^{Asn} (^{34}GUU^{36}) similarly differ in the third base, as described for tRNA^{Glu} and tRNA^{Gln} (see above). Discrimination in AspRS therefore involves two pyrimidines, cytosine and uracil, that differ only in the functional group at atom C4. In these class II synthetases, neither related in sequence nor in structure to GluRS,[27] recognition of cognate

tRNA exclusively involves the anticodon-binding domain. Discriminating and non-discriminating AspRS mainly differ with respect to the so-called L1 loop involved in recognizing the third anticodon nucleotide.[28] This loop is mostly five to seven residues longer in discriminating AspRS. A conserved proline in this loop was also found to be essential for mischarging AspRS,[28,29] while a histidine and a glycine (His31 and Gly83 in *Pseudomonas aeruginosa*) were identified to be conserved in non-discriminating, bacterial AspRS.[30]

The mechanisms that have evolved to switch from non-discriminating to discriminating synthetases are thus fundamentally unrelated for GluRS and AspRS. In GluRS the introduction of an arginine in position 366 and a glutamate in position 443 appear sufficient to ensure discrimination. No insertions, deletions or large conformational changes are required. Hence, the observation that enzymes of *Thermus/Deinococcus* and proteobacteria are individually more closely related to non-discriminating GluRS than to each other may indicate that this principle of GluRS discrimination may have evolved more than once.

Materials and Methods

Cloning, production and purification of GluRS

The gene for GluRS (gltX) of *T. elongatus* strain BP-1 was amplified from genomic DNA and cloned into the NdeI/XhoHI sites of the *E. coli* expression vector pET29 (Novagen). The resulting plasmid encodes ND-GluRS$_{Tel}$ with a native N terminus and a C-terminal His-tag. Transformed *E. coli* BL21 CodonPlus cells (Stratagene) were cultivated at 37 °C to A_{600} of 0.6 in LB-medium with 30 μg/ml of kanamycin and 50 μg/ml of chloramphenicol. The temperature was lowered to 20 °C, protein expression induced with 100 μM isopropyl-β-D-thiogalactopyranoside, and the cells cultivated for 20 h. Cells were centrifuged, disrupted by French press and cell debris removed by centrifugation at 4 °C. ND-GluRS$_{Tel}$ was isolated from the soluble fraction by Ni-NTA affinity chromatography and purified by anion exchange chromatography (MonoQ HR 10/10; GE Healthcare) using a linear gradient 10 mM to 400 mM NaCl in 20 column volumes in 20 mM Hepes (pH 7.9), 2 mM DTT and 250 μM $MgCl_2$. GluRS fractions were pooled and concentrated by a 10 kDa cut-off Vivaspin centrifugal concentrator (Vivascience) and further purified using a Superdex 75 26/60 gel filtration column (GE Healthcare) in 20 mM Hepes (pH 7.9), 20 mM NaCl, 10 mM DTT and 250 μM $MgCl_2$ at a flow rate of 2 ml/min. Purified ND-GluRS$_{Tel}$ was concentrated to 3 mg/ml. The overall yield was ~10 mg protein/l of bacterial culture. Protein integrity and purity were verified by SDS–PAGE, N-terminal protein sequencing, dynamic light scattering and mass-spectrometry.

Cultivation of *T. elongatus* and preparation of cell free extracts

T. elongatus BP1 cells were cultivated in DTN-medium supplemented with micronutrients in 10% (v/v) CO_2-enriched atmosphere at 55 °C in a 5l fermenter under continuous white light illumination (~80 μmol of photons·m^{-2}s^{-1}) to an A_{800} of 2.0.[31] Harvesting by centrifugation yielded 1.5 g wet cell mass/l culture. A total of 17 g of cells were washed in 50 mM Tris–HCl (pH 7.5), 10 mM magnesium acetate, 3 mM DTT and 1.5 mg/l of RNaseOut (Invitrogen, Karlsruhe, Germany). The cells were ruptured by sonification using a sonotrode (HD 2070 and MS73 tip; Bandelin, Berlin, Germany). The soluble fraction was obtained by ultracentrifugation at 4 °C and 100,000*g*.

Isolation of tRNA^{Glu} and tRNA^{Gln} from *T. elongatus*

Mature tRNA^{Glu} and tRNA^{Gln} from *T. elongatus* were obtained by acidic phenol extraction as described.[32] The tRNA extracted from 200 mg of total RNA was purified by anion exchange chromatography using the Q500 Maxi Kit (Qiagen, Hilden, Germany). Nine milligram of total tRNA was deacylated by incubation at 37 °C for 1 h in the presence of 200 mM Tris-acetate (pH 9.0). Deacylated tRNAs were recovered by ethanol precipitation.[33]

tRNA purification

Mature tRNA^{Gln} and tRNA^{Glu} from *T. elongatus* were isolated by an improved solid-phase DNA probe method ("chaplet" column chromatography).[34] A total of 150 μg of 5′-biotinylated, gel-purified DNA oligonucleotides, complementary to the target tRNA was bound to streptavidin beads (Pierce) in 10 mM Tris–HCl (pH 7.5). 5′-biotin-CCCGCTGCCTAACCGCTTGGCGACACCCCA-3′ for tRNA^{Gln} and 5′-biotin-GGAGGTGTCCTAGGCCACTA-GACGATGGGGGC-3′ for tRNA^{Glu} (Biomers·net GmbH, Ulm, Germany). Beads were equilibrated in 6× NTE solution (20× NTE: 4 M NaCl, 0.1 M Tris–HCl (pH 7.5), 50 mM EDTA, 5 mM β-mercaptoethanol). A total of 10 mg unfractionated *T. elongatus* tRNA (10 mg/ml in 6× NTE) were added, incubated at 65 °C for 30 min, and allowed to cool to 30 °C. Beads were washed three times in 3× NTE, twice in 1× NTE and once in 0.1× NTE. tRNAs were eluted with 0.1× NTE at 65–68 °C, ethanol-precipitated and redissolved in amino acylation buffer (50 mM Hepes (pH 7.5), 25 mM KCl, 15 mM $MgCl_2$, 5 mM DTT). Further purification was achieved using the QIAquick nucleotide removal kit (Qiagen, Hilden, Germany).

The purity of tRNAs was controlled by Northern dot-blot-analysis. A total of 0.5 −1 μg tRNA was crosslinked onto a nylon membrane by UV irradiation and incubated with biotinylated oligonucleotides in 250 mM Na_2HPO_4, 1 mM EDTA, 20% (w/v) SDS, 100 mM maleic acid, 150 mM NaCl and blocking reagent (Roche 1096176) overnight at pH 7.5 and 68 °C. After rinsing five times in PBS (137 mM NaCl, 2.2 mM KCl, 10 mM Na_2HPO_4, 1.7 mM KH_2PO_4 (pH 7.4)) and 0.1% (v/v) Tween 20, streptavidin-AP-conjugate (IBA BioTAGnology, Göttingen, Germany) was added to the membrane and incubated for 90 min at 37 °C, washed 3× in PBS plus 0.1% Tween 20. The color reaction was performed using nitroblue tetrazolium chloride (NBT) and 5-bromo,4-chloro,3-indolylphosphate (BCIP) (Roth, Karlsruhe, Germany). Degradation of tRNAs was checked by denaturing 12% (w/v) polyacrylamide/8M urea gel electrophoresis.

Aminoacylation assays with GluRS

In vitro acylation experiments with ND-GluRS$_{Tel}$ were carried out at 37 °C in a 130 μl reaction mixture containing

50 mM Hepes (pH 7.5), 25 mM KCl, 15 mM $MgCl_2$, 5 mM DTT, 5 mM ATP, 30 μM L-[^{14}C]Glu (237 mCi/ mmol) and 21 to 0.7 μg of pure tRNA. The reactions were started by addition of the enzyme (1.8 μM GluRS). Samples (15 μl) were taken at different times, spotted on 3 MM Whatman filter paper discs and washed twice in 10%, once in 5% (w/v) trichloroacetic acid and finally in ethanol. Uniformly labeled L-[^{14}C]Glu (237 mCi/ mmol) and L-[^{14}C]Gln (210 mCi/mmol) were purchased from Hartmann Analytic (Braunschweig, Germany).

Crystallization

ND-GluRS$_{Tel}$ was crystallized by hanging drop vapor diffusion at 20 °C. Three μl of protein (3 mg/ml in 20 mM Hepes (pH 7.9), 20 mM NaCl, 10 mM DTT, 250 μM zinc acetate and 250 μM $MgCl_2$) was added to 3 μl of reservoir solution (740 mM sodium citrate, 140 mM citric acid (pH 5.8) and 10 mM DTT). Crystals grew to a size of 500 μm × 100 μm × 50 μm within one to two weeks. Prior to X-ray data collection 25% (v/v) of a 50% (w/v) trehalose solution were added for cryo-protection. Crystals belong to space group $P2_1$ with cell constants $a = 36.2$ Å, $b = 99.6$ Å and $c = 182.4$ Å. A V_M-value of 2.97 Å^3/Da[35] indicates the presence of two GluRS molecules per asymmetric unit, corresponding to a solvent content of 59%.

Data collection, structure determination and analysis

X-ray diffraction data were collected at the beamline PX I (Swiss Light Source). Data were processed and scaled using the XDS program package.[36] The structure of GluRS from *T. thermophilus* (PDB code 1GLN)[11] served as model in molecular replacement using Phaser.[37] CNS[38] was used for rigid-body and simulated annealing refinement, REFMAC5[39] for subsequent refinement, including TLS protocols. Coot was used for manual model building and structural analysis.[40] The structure was validated using WHAT IF[41] and PROCHECK.[42] Molecular depictions were prepared using PyMOL†. LSQKAB of the CCP4 program suite[43] was used to calculate root-mean-square deviations. Sequence alignments were performed with CLUSTAL W.[44]

Protein Data Bank accession number

The coordinates of the structure have been deposited in the RCSB Protein Data Bank (entry code: 2CFO).

Acknowledgements

We gratefully acknowledge synchrotron beam time at the Swiss Light Source, Paul Scherrer Institut, Villigen, Switzerland. This work was funded by the Deutsche Forschungsgemeinschaft (DFG) to D.W.H. (He 1852/5-3) and D.J. (Ja 470/7-3). D.W.H. acknowledges support from the Fonds der Chemischen Industrie.

† http://www.pymol.sourceforge.net

References

1. Eriani, G., Delarue, M., Poch, O., Gangloff, J. & Moras, D. (1990). Partition of tRNA synthetases into two classes based on mutually exclusive sets of sequence motifs. *Nature*, **347**, 203–206.
2. Sekine, S., Nureki, O., Dubois, D. Y., Bernier, S., Chenevert, R., Lapointe, J. *et al.* (2003). ATP binding by glutamyl-tRNA synthetase is switched to the productive mode by tRNA binding. *EMBO J.* **22**, 676–688.
3. Ibba, M. & Söll, D. (2000). Aminoacyl-tRNA synthesis. *Ann. Rev. Biochem.* **69**, 617–650.
4. Ibba, M. & Söll, D. (2001). The renaissance of aminoacyl-tRNA synthesis. *EMBO Rep.* **2**, 382–387.
5. Curnow, A. W., Ibba, M. & Söll, D. (1996). tRNA-dependent asparagine formation. *Nature*, **382**, 589–590.
6. Sauerwald, A., Zhu, W., Major, T. A., Roy, H., Palioura, S., Jahn, D. *et al.* (2005). RNA-dependent cysteine biosynthesis in Archaea. *Science*, **307**, 1969–1972.
7. White, B. N. & Bayley, S. T. (1972). Further codon assignments in an extremely halophilic bacterium using a cell-free protein-synthesizing system and a ribosomal binding assay. *Can. J. Biochem.* **50**, 600–609.
8. Schön, A., Kannangara, C. G., Gough, S. & Söll, D. (1988). Protein biosynthesis in organelles requires misaminoacylation of tRNA. *Nature*, **331**, 187–190.
9. Lapointe, J., Duplain, L. & Proulx, M. (1986). A single glutamyl-tRNA synthetase aminoacylates tRNAGlu and tRNAGln in *Bacillus subtilis* and efficiently misacylates *Escherichia coli* tRNAGln1 in vitro. *J. Bacteriol.* **165**, 88–93.
10. Lapointe, J. (1982). Study of the evolution of the genetic code by comparing the structural and catalytic properties of the aminoacyl-tRNA synthetases. *Can. J. Biochem.* **60**, 471–474.
11. Nureki, O., Vassylyev, D. G., Katayanagi, K., Shimizu, T., Sekine, S., Kigawa, T. *et al.* (1995). Architectures of class-defining and specific domains of glutamyl-tRNA synthetase. *Science*, **267**, 1958–1965.
12. Brown, J. R. & Doolittle, W. F. (1999). Gene descent, duplication, and horizontal transfer in the evolution of glutamyl- and glutaminyl-tRNA synthetases. *J. Mol. Evol.* **49**, 485–495.
13. Lamour, V., Quevillon, S., Diriong, S., N'Guyen, V., Lipinski, M. & Mirande, M. (1994). Evolution of the Glx-tRNA Synthetase Family: The Glutaminyl Enzyme as a Case of Horizontal Gene Transfer. *PNAS*, **91**, 8670–8674.
14. Nakamura, Y., Kaneko, T., Sato, S., Ikeuchi, M., Katoh, H., Sasamoto, S. *et al.* (2002). Complete genome structure of the thermophilic cyanobacterium *Thermosynechococcus elongatus* BP-1. *DNA Res.* **9**, 123–130.
15. Lee, J. & Hendrickson, T. L. (2004). Divergent anticodon recognition in contrasting Glutamyl-tRNA Synthetases. *J. Mol. Biol.* **344**, 1167–1174.
16. Curnow, A. W., Hong, K.-W., Yuan, R., Kim, S.-I., Martins, O., Winkler, W. *et al.* (1997). Glu-tRNA^{Gln} amidotransferase: a novel heterotrimeric enzyme required for correct decoding of glutamine codons during translation. *PNAS*, **94**, 11819–11826.
17. Randau, L., Münch, R., Hohn, M. J., Jahn, D. & Söll, D. (2005). *Nanoarchaeum equitans* creates functional tRNAs from separate genes for their 5′- and 3′-halves. *Nature*, **433**, 537–541.
18. Rogers, K. C. & Söll, D. (1993). Discrimination among tRNAs intermediate in glutamate and glutamine acceptor identity. *Biochemistry*, **32**, 14210–14219.

19. Becker, H. D. & Kern, D. (1998). *Thermus thermophilus*: a link in evolution of the tRNA-dependent amino acid amidation pathways. *PNAS*, **95**, 12832–12837.
20. Rould, M. A., Perona, J. J., Söll, D. & Steitz, T. A. (1989). Structure of *E. coli* glutaminyl-tRNA synthetase complexed with tRNA(Gln) and ATP at 2.8 Å resolution. *Science*, **246**, 1135–1142.
21. Liu, J., Gagnon, Y., Gauthier, J., Furenlid, L., L'Heureux, P.-J., Auger, M. *et al.* (1995). The zinc-binding site of *Escherichia coli* glutamyl-tRNA synthetase is located in the acceptor-binding domain. *J. Biol. Chem.* **270**, 15162–15169.
22. Banerjee, R., Dubois, D. Y., Gauthier, J., Lin, S.-X., Roy, S. & Lapointe, J. (2004). The zinc-binding site of a class I aminoacyl-tRNA synthetase is a SWIM domain that modulates amino acid binding via the tRNA acceptor arm. *Eur. J. Biochem.* **271**, 724–733.
23. Siatecka, M., Rozek, M., Barciszewski, J. & Mirande, M. (1998). Modular evolution of the Glx-tRNA synthetase family. Rooting of the evolutionary tree between the bacteria and archaea/eukarya branches. *Eur. J.Biochem.* **256**, 80–87.
24. Sekine, S., Nureki, O., Shimada, A., Vassylyev, D. G. & Yokoyama, S. (2001). Structural basis for anticodon recognition by discriminating glutamyl-tRNA synthetase. *Nature Struct. Biol.* **8**, 203–206.
25. Madore, E., Florentz, C., Giege, R., Sekine, S., Yokoyama, S. & Lapointe, J. (1999). Effect of modified nucleotides on *Escherichia coli* $tRNA^{Glu}$ structure and on its aminoacylation by glutamyl-tRNA synthetase. Predominant and distinct roles of the mnm5 and s2 modifications of U34. *Eur. J. Biochem.* **266**, 1128–1135.
26. Rould, M. A., Perona, J. J. & Steitz, T. A. (1991). Structural basis of anticodon loop recognition by glutaminyl-tRNA synthetase. *Nature*, **352**, 213–218.
27. Carter, C. W., Jr (1993). Cognition, mechanism, and evolutionary relationships in aminoacyl-tRNA synthetases. *Annu. Rev. Biochem.* **62**, 715–748.
28. Charron, C., Roy, H., Blaise, M., Giege, R. & Kern, D. (2003). Non-discriminating and discriminating aspartyl-tRNA synthetases differ in the anticodon-binding domain. *EMBO J.* **22**, 1632–1643.
29. Feng, L., Yuan, J., Toogood, H., Tumbula-Hansen, D. & Söll, D. (2005). Aspartyl-tRNA synthetase requires a conserved proline in the anticodon-binding loop for $tRNA^{Asn}$ recognition in vivo. *J. Biol. Chem.* **280**, 20638–20641.
30. Bernard, D., Akochy, P.-M., Beaulieu, D., Lapointe, J. & Roy, P. H. (2006). Two residues in the anticodon recognition domain of the Aspartyl-tRNA synthetase from *Pseudomonas aeruginosa* are individually implicated in the recognition of $tRNA^{Asn}$. *J. Bacteriol.* **188**, 269–274.
31. Zouni, A., Witt, H.-T., Kern, J., Fromme, P., Krauss, N., Saenger, W. & Orth, P. (2001). Crystal structure of photosystem II from *Synechococcus elongatus* at 3.8 Å resolution. *Nature*, **409**, 739–743.
32. Sambrook, J., Fritsch, E. F. & Maniatis, T. (1989). *Molecular cloning: A Laboratory Manual*, 2nd edit., Cold Spring Harbor Laboratory Press, Cold Spring Harbor NY.
33. Curnow, A. W., Tumbula, D. L., Pelaschier, J. T., Min, B. & Söll, D. (1998). Glutamyl-$tRNA^{Gln}$ amidotransferase in *Deinococcus radiodurans* may be confined to asparagine biosynthesis. *PNAS*, **95**, 12838–12843.
34. Kaneko, T., Suzuki, T., Kapushoc, S. T., Rubio, M. A., Ghazvini, J., Watanabe, K. & Simpson, L. (2003). Wobble modification differences and subcellular localization of tRNAs in *Leishmania tarentolae*: implication for tRNA sorting mechanism. *EMBO J.* **22**, 657–667.
35. Matthews, B. W. (1968). Solvent content of protein crystals. *J. Mol. Biol.* **33**, 491–497.
36. Kabsch, W. (1993). Automatic processing of rotation diffraction data from crystals of initially unknown symmetry and cell constants. *J. Appl. Crystallog.* **26**, 795–800.
37. McCoy, A. J., Grosse-Kunstleve, R. W., Storoni, L. C. & Read, R. J. (2005). Likelihood-enhanced fast translation functions. *Acta Crystallog. sect. D*, **61**, 458–464.
38. Brünger, A. T., Adams, P. D., Clore, G. M., DeLano, W. L., Gros, P., Grosse-Kunstleve, R. W. *et al.* (1998). Crystallography and NMR system: A new software suite for macromolecular structure determination. *Acta Crystallog. sect. D*, **54**, 905–921.
39. Murshudov, G. N., Vagin, A. A. & Dodson, E. J. (1997). Refinement of macromolecular structures by the maximum-likelihood method. *Acta Crystallog. sect. D*, **53**, 240–255.
40. Emsley, P. & Cowtan, K. (2004). Coot: model-building tools for molecular graphics. *Acta Crystallog. sect. D*, **60**, 2126–2132.
41. Vriend, G. (1990). WHAT IF: a molecular modeling and drug design program. *J. Mol. Graph.* **8**, 52–56.
42. Laskowski, R. A., MacArthur, M. W., Moss, D. S. & Thornton, J. M. (1993). PROCHECK: a program to check the stereochemical quality of protein structures. *J. Appl. Crystallog.* **26**, 283–291.
43. Collaborative Computational Project, N. (1994). The CCP4 suite: programs for protein crystallography. *Acta Crystallog. sect. D*, **50**, 760–763.
44. Thompson, J. D., Higgins, D. G. & Gibson, T. J. (1994). CLUSTAL W: improving the sensitivity of progressive multiple sequence alignment through sequence weighting, position-specific gap penalties and weight matrix choice. *Nucl. Acids Res.* **22**, 4673–4680.

Edited by K. Morikawa

(Received 16 May 2006; received in revised form 20 June 2006; accepted 21 June 2006)
Available online 5 July 2006